Preconditioning with acteoside ameliorates myocardial ischemia-reperfusion injury by targeting HSP90AA1 and the PI3K/Akt signaling pathway

JING LI[1*], YUXIN GUO[1*], YANG YANG[1], QING XUE[2], HONG CAO[2], GUANGYUAN YANG[2], LINLIN JIA[1,3] and HAIBO YU[2]

[1]Department of Physiology, Basic Medical College, Jiamusi University, Jiamusi, Heilongjiang 154000, P.R. China; [2]Department of Cardiology, The First Affiliated Hospital to Jiamusi University, Jiamusi, Heilongjiang 154000, P.R. China; [3]Department of Medical Nursing, Nursing College, Zhangzhou Health Vocational College, Zhangzhou, Fujian 363000, P.R. China

Received September 25, 2024; Accepted December 18, 2024

DOI: 10.3892/mmr.2025.13442

Abstract. The present study aimed to investigate the cardioprotective effects of acteoside (AC) on myocardial ischemia-reperfusion injury (MIRI). To meet this aim, a network pharmacological analysis was conducted to search for key genes and signaling pathways associated with AC and MIRI. The infarct size of the rat heart was evaluated using 2,3,5-triphenyltetrazolium chloride staining, and the serum levels of creatine kinase MB isoenzyme, cardiac troponin I, malondialdehyde and superoxide dismutase were subsequently detected in an *in vivo* experiment. The inhibitory effect of AC on oxidative stress was further confirmed by assessing the intracellular accumulation of reactive oxygen species (ROS). Hematoxylin and eosin staining was subsequently carried out to observe cardiac histopathological damage. The anti-apoptotic effects of AC were determined using terminal deoxynucleotidyl-transferase-mediated dUTP nick end labeling assay and Hoechst 33342 staining, and the expression levels of apoptosis-associated proteins in the myocardial tissue were assessed using immunohistochemical analysis. In addition, cell viability was determined using a Cell Counting Kit-8 assay, and the expression levels of key target proteins associated with AC and MIRI were detected by western blot analysis. The results suggested that pretreatment with AC could mitigate MIRI-induced myocardial damage, oxidative stress and apoptosis. The anti-apoptotic effects of AC were associated with elevated Bcl-2 levels, and reduced caspase-3 and Bax expression levels in myocardial tissue. *In vitro*, AC pretreatment both led to an increased rate of cell survival and alleviated oxidative stress, as demonstrated by a decreased level of intracellular ROS accumulation. Moreover, guided by the network pharmacological analysis, heat-shock protein 90AA1 (HSP90AA1) and the phosphoinositide 3-kinase (PI3K)/serine-threonine protein kinase (Akt) signaling pathway emerged as key targets for the action of AC against MIRI. Furthermore, the western blot analysis results showed that pretreatment with AC led to a significant increase in the activity of the PI3K/Akt signaling pathway, in addition to increased expression levels of glycogen synthase kinase-3β and HSP90AA1. Taken together, the findings of the present study revealed that AC may exert cardioprotective effects on MIRI through suppressing apoptosis and oxidative stress by regulating the expression and activity of key proteins.

Introduction

Myocardial ischemia (MI) occurs when there is an interruption of blood supply to the heart. The restoration of blood flow to the ischemic myocardium results in more severe damage compared with that prior to reperfusion, this is known as MI-reperfusion injury (MIRI). MIRI may occur during the recovery phases of various cardiovascular diseases, including those associated with coronary artery bypass surgery, coronary angioplasty or thrombolysis, heart transplantation and open-heart surgery (1,2). Patients with MIRI typically experience a worsening of symptoms, including a sudden drop in blood pressure, cardiac dysfunction, arrhythmias and even sudden death (3). MIRI has become a considerable concern in the treatment of MI, as it can worsen the outcome of patients. The underlying mechanisms responsible for MIRI are complex, multi-factorial and interconnected. Oxidative stress, intracellular calcium overload, energy metabolism disorders, apoptosis, endoplasmic reticulum stress, disruption of the

Correspondence to: Professor Haibo Yu, Department of Cardiology, The First Affiliated Hospital to Jiamusi University, 348 Dexiang Street, Jiamusi, Heilongjiang 154000, P.R. China
E-mail: yu118119@163.com

Professor Linlin Jia, Department of Medical Nursing, Nursing College, Zhangzhou Health Vocational College, 29 Xiyangping Road, Xiangcheng, Zhangzhou, Fujian 363000, P.R. China
E-mail: 17504582110@163.com

*Contributed equally

Key words: myocardial ischemia-reperfusion injury, acteoside, HSP90AA1, PI3K/Akt signaling pathway, GSK-3β

mitochondrial membrane potential and the interplay among these various factors all contribute to endothelial injury and cell death in MIRI (4,5).

Acteoside (AC), also known as verbascoside or kusaginin, is a natural phenolic glycoside that is commonly found in several species of plant, such as *Cistanche deserticola* and *Rehmannia glutinosa*. Owing to its natural, safe and effective properties, AC may be used as an additive to enhance the nutritional value and health benefits of food (6,7). AC possesses multiple pharmacological properties, including anti-oxidative, anti-inflammatory, antitumor, anti-aging, cardioprotective, neuroprotective and cartilage-protective properties (8,9). Our previous findings revealed that, in a rat model of MIRI, pretreatment with AC was able to alleviate pain, attenuate pathological changes in the myocardial structure, and reduce the serum levels of cardiac enzymes and noradrenaline. These protective effects of AC were found to be mediated by inhibiting oxidative stress and reducing the apoptosis of cardiomyocytes (Li *et al*, unpublished data).

To further investigate the complex mechanisms underlying the action of AC against MIRI, the present study used network pharmacological analysis, which identified heat shock protein 90AA1 (HSP90AA1) as an important target. HSP90 is an abundant protein that has a key role in cells and carries out a diverse range of functions (10,11). HSP90AA1 is a fundamental and highly conserved molecular chaperone belonging to the HSP90 family of proteins. HSP90AA1 fulfills a key role, both in terms of maintaining cellular homeostasis and in regulating a number of cellular processes, including protein folding, protein stability and protein degradation. It also participates in signaling pathways involved in cell proliferation, differentiation, survival and apoptosis (12,13). In addition to HSP90AA1, the phosphoinositide 3-kinase (PI3K)/serine-threonine protein kinase (Akt) signaling pathway has emerged as a key target of AC against MIRI. The PI3K/Akt signaling pathway exerts protective effects in MIRI via inhibiting apoptosis, promoting cell survival and proliferation, regulating energy metabolism and mitigating inflammatory responses (14,15). Drugs that activate the PI3K/Akt signaling pathway have shown promise in ameliorating MIRI (16,17). Furthermore, ischemic or pharmacological preconditioning has been shown to activate the PI3K/Akt signaling pathway, thereby providing protection against subsequent MIRI (18).

Using network pharmacological analysis, the present study aimed to first screen and analyze the key genes and signaling pathways that are associated with AC and MIRI. Molecular docking was subsequently used to validate the interaction between AC and the key target proteins. MIRI models using Sprague-Dawley (SD) rats and H9c2 cells were then established to further confirm the cardioprotective effects of AC. Finally, the protein levels of HSP90AA1, PI3K, Akt and glycogen synthase kinase-3β (GSK-3β), which acts downstream of Akt, were assessed using a series of *in vivo* and *in vitro* experiments.

Materials and methods

Ethics statement. All experimental protocols carried out in the present study were approved by the Biology and Animal Ethical Committee of the Basic Medical College, Jiamusi University (approval no. JDJCYXY-2024-0021; Jiamusi, China), and were conducted in accordance with the Guide for the Care and Use of Laboratory Animals published by the National Institutes of Health (19). An outline of the general protocol of the present study is shown in Fig. 1.

Network pharmacological analysis: Identification of key targets associated with both AC and MIRI. Targets for AC were sourced and screened through a search of databases, including the Swiss Target Prediction (http://www.swisstargetprediction.ch/) and Similarity Ensemble Approach (https://sea.bkslab.org/) databases, by inputting the Simplified Molecular Input Line Entry System for AC. Following data refinement, duplicative genes were highlighted and the gene names were retrieved from the UniProt (https://www.uniprot.org/) database. Genes associated with MIRI were subsequently identified and selected from the GeneCards (https://www.genecards.org/) and DisGeNET (https://www.disgenet.org/) databases. The genes retrieved from both databases were selected as the MIRI-associated genes. Finally, comparing among the retrieved AC targets and the MIRI-associated genes, overlapping targets were identified for further downstream analysis.

Construction of the protein-protein interaction (PPI) network. Overlapping target genes were inputted into the Search Tool for the Retrieval of Interacting Genes/Proteins (STRING 12.0; https://string-db.org), with the species selected as 'Homo sapiens' to obtain the PPI interaction network. Cytoscape (version 3.7.0) software (https://cytoscape.org/) was subsequently used for visualization of the PPI network. In the PPI network, nodes and edges represent proteins and their interactions, respectively.

Gene ontology (GO) and kyoto encyclopedia of genes and genomes (KEGG) pathway enrichment analyses. After having identified the intersecting target genes between AC and MIRI, GO and KEGG pathway enrichment analyses were carried out using the DAVID v2024q2 database (https://david.ncifcrf.gov/), with $P<0.05$ selected as the cut-off criterion. The online platform of Microbiome Informatics (https://www.bioinformatics.com.cn/basic_local_go_pathway_enrichment_analysis_122) was used to create bar charts to display the results of the GO term enrichment analysis, and bubble plots were constructed to show the results of the KEGG pathway enrichment analysis.

Construction of the AC-key target genes/pathways-MIRI network. Cytoscape software was used for visualization of the AC-key target genes/pathways-MIRI network.

Molecular docking analysis. PubChem (https://pubchem.ncbi.nlm.nih.gov/) and Protein Data Bank (https://www.rcsb.org/) databases were used to obtain the 3D structure of AC and the protein structures of the key targets. Autodock Vina software 1.1.2 (The Scripps Research Institute; https://vina.scripps.edu/downloads/) was subsequently used for molecular docking analysis.

AC preconditioning. A total of 45 male SD rats (age, 8 weeks; body weight, 230-250 g) were obtained from the Experimental Animal Center of the Second Hospital Affiliated to Harbin

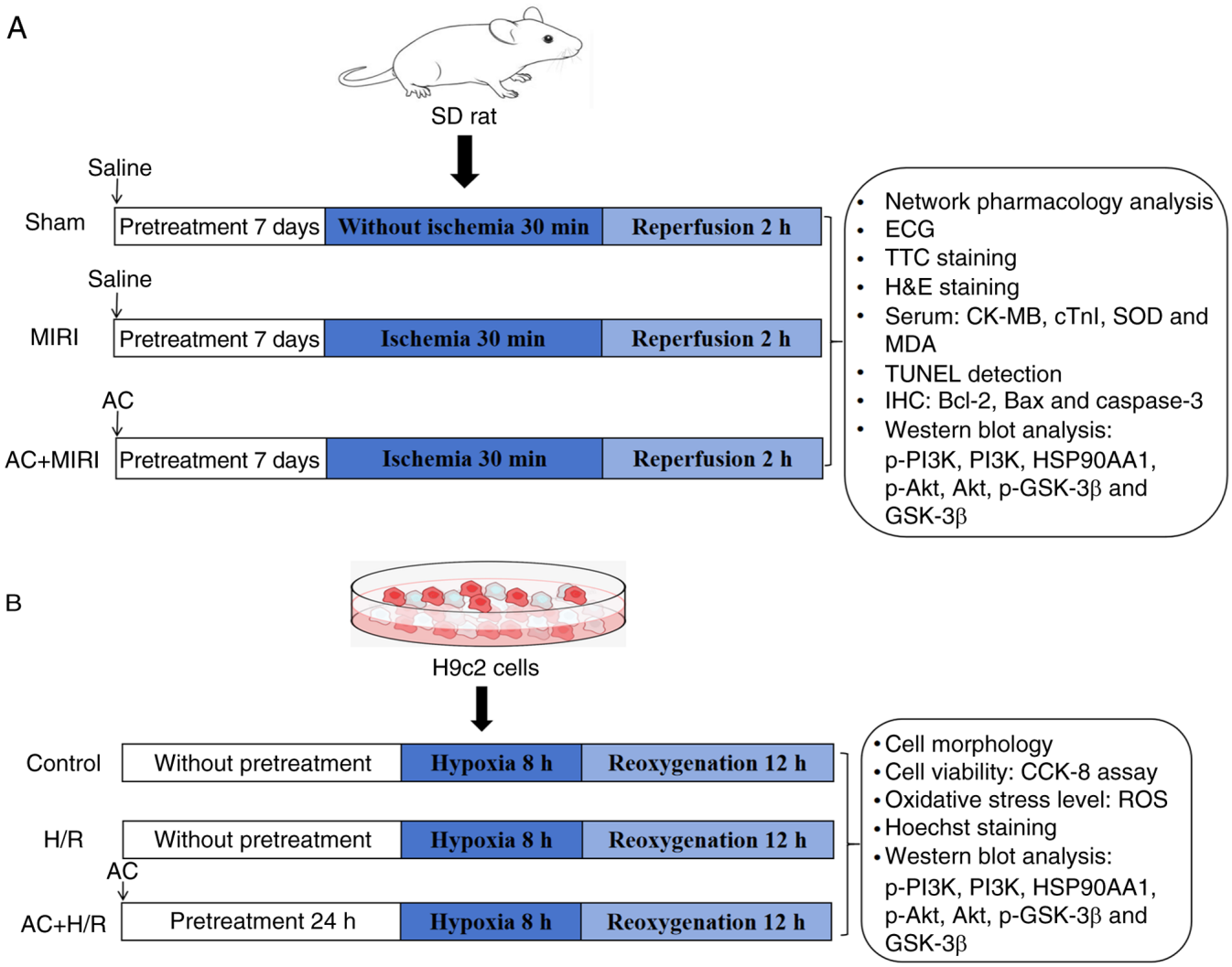

Figure 1. General protocol of the present study. (A) Illustrative diagrams and measurements acquired from Sprague-Dawley rats. (B) Illustrative diagrams and measurements acquired from H9c2 cells. MIRI, myocardial ischemia-reperfusion injury; AC, acteoside; ECG, electrocardiogram; TTC, 2,3,5-triphenyltetrazolium chloride; H&E, hematoxylin and eosin; CK-MB, creatine kinase MB isoenzyme; cTnI, cardiac troponin I; MDA, malondialdehyde; SOD, superoxide dismutase; TUNEL, terminal deoxynucleotidyl-transferase-mediated dUTP nick end labeling; IHC, immunohistochemistry; p-, phosphorylated; PI3K, phosphoinositide 3-kinase; HSP90AA1, heat-shock protein 90AA1; Akt, serine-threonine protein kinase; GSK-3β, glycogen synthase kinase-3β; CCK-8, Cell Counting Kit-8; H/R, hypoxia/reoxygenation; ROS, reactive oxygen species.

Medical University (Harbin, China). Considerations for animal welfare included making every possible effort to alleviate suffering and distress, alongside the utilization of anesthetics and the implementation of controlled living environments. The rats were housed under standard conditions (temperature, 24.0±2.0˚C; humidity, 40-60%; a 12-h light/dark cycle) with unrestricted access to food and water. To ensure a sanitary environment, the bedding was replaced every 2 days. After 7 days of adaptive feeding, the rats were evenly and randomly divided into three groups, namely the Sham group (n=15), the MIRI group (n=15) and the AC + MIRI group (n=15). The rats in the AC + MIRI group were intragastrically administered 80 mg/kg AC once daily for 7 days, whereas the rats in the other two groups intragastrically received a volume of 1 ml/100 g water. AC was purchased from Jiangsu Yongjian Pharmaceutical Technology Co., Ltd. and was dissolved in saline solution.

Establishment of the MIRI rat model. The duration of the experiment was ~5 h including the operation preparation, anesthesia, establishment of MIRI, specimen collection and euthanasia of animals [intraperitoneal injection of 1% sodium pentobarbital (150 mg/kg)]. Animal health and behavior were monitored during the whole experiment. If a rat displayed persistent signs of distress, such as respiratory distress, convulsions, or continuous and severe abnormalities in electrocardiogram (ECG) recordings, immediate euthanasia was carried out Thoracotomies were conducted in rats after they had been anesthetized with 2% isoflurane, as previously described (20). The left anterior descending (LAD) coronary artery was blocked using a 6-0 silk suture for 30 min, followed by 120 min of reperfusion. The presence of MI was verified according to the elevation of the ST segment, as it appeared on an ECG. The rats in the Sham group underwent an identical surgical procedure, but without the occlusion of the artery. In the present study, during the reperfusion phase, one rat in the MIRI group underwent euthanasia as aforementioned due to severe arrhythmias. Successful euthanasia was confirmed through monitoring the cessation of respiration, heartbeat and pupil dilation (21).

Evaluation of the infarct size in MIRI. After having established the MIRI rat model, 2,3,5-triphenyltetrazolium chloride (TTC) staining was used to evaluate the infarct size. The rats were sacrificed under anesthesia via the intraperitoneal injection of 1% sodium pentobarbital at a dose of 150 mg/kg, as previously described (21), and their hearts were harvested and frozen for slicing. Subsequently, the hearts were cut into five 2-mm^3 slices, and incubated in TTC solution (Nanjing Jiancheng Bioengineering Institute) in the dark at 37˚C for 30 min, before being preserved in 4% paraformaldehyde (PFA) overnight at 4˚C. The infarct tissue was found to exhibit a distinct white color, in contrast with the viable tissue, which was stained red. The infarct size was analyzed using Image-Pro Plus (version 6.0; Media Cybernetics, Inc.), and the results were expressed as the percentage of infarct area relative to the entire area.

Biochemical detection of the levels of serum markers. For serum collection, the rats were placed in an induction chamber and received 3% isoflurane; respiration, heart rate and muscle relaxation were assessed to ensure an appropriate depth of anesthesia. Subsequently, the rats were transferred to an operating table and anesthesia was maintained using 2% isoflurane. Whole blood (400-500 μl) was then obtained from the abdominal aorta, which was used to yield 300-400 μl serum. After blood collection, the rats were was immediately euthanized (20). Whole blood samples were centrifuged at 15,000 x g for 25 min at 4˚C and the supernatant was extracted. Subsequently, myocardial injury markers were analyzed in the supernatant by ELISA. Serum levels of creatine kinase MB isoenzyme (CK-MB) and cardiac troponin I (cTnI) were analyzed using their respective ELISA kits (cat. nos. H197-1-1 and H149-2-2; Nanjing Jiancheng Bioengineering Institute), following the manufacturer's instructions. The concentrations of malondialdehyde (MDA) and superoxide dismutase (SOD) in the serum were also quantified using the corresponding biochemical assay kits (cat. nos. A003-1-2 and A001-3-2; Nanjing Jiancheng Bioengineering Institute), following the manufacturer's protocols.

Histological analysis. Hematoxylin and eosin (H&E) staining was performed to observe the extent of cardiac histopathological damage. Following reperfusion for 120 min, the hearts were collected and preserved in 4% PFA for 24 h at room temperature. Subsequently, the myocardial tissue of the ventricles underwent routine H&E staining. After undergoing the standard alcohol-xylene treatment procedure, the ventricular tissues were embedded within paraffin wax blocks. Paraffin-embedded sections (4 μm) were then mounted onto slides, and were stained with hematoxylin and eosin for 10 min at room temperature. Finally, histological images were captured under an optical microscope (E200MV microscope; Nikon Corporation).

Terminal deoxynucleotidyl-transferase-mediated dUTP nick end labeling (TUNEL) staining. Apoptosis of cardiomyocytes in the ventricular tissues was subsequently detected by observing the cells using fluorescence microscopy with an Olympus IX71 microscope (Olympus Corporation), with the application of a TUNEL assay kit (cat. no. G1504; Wuhan Servicebio Technology Co., Ltd.), following the manufacturer's instructions. The percentages of apoptotic cells were determined by calculating the ratio of TUNEL-positive cells to the total number of cells, with five focal planes being analyzed for each group. Briefly, TUNEL staining was performed as follows: Paraffin-embedded sections were washed three times with PBS (pH 7.4) for 5 min each time. After PBS was removed, DAPI dye solution (cat. no. G1012; Wuhan Servicebio Technology Co., Ltd.) was added and incubated at room temperature for 10 min in the dark. The slide was then placed in PBS (pH 7.4) and washed three times with agitation (5 min each).

Immunohistochemical analysis. Levels of apoptosis-associated proteins in the myocardial tissue, including Bcl-2 (1:100; cat. no. BA0412; Wuhan Boster Biological Technology Co., Ltd.), Bax (1:100; cat. no. A00183; Wuhan Boster Biological Technology Co., Ltd.) and caspase-3 (1:100; cat. no. M00334-9; Wuhan Boster Biological Technology Co., Ltd.), were determined by immunohistochemical analysis. Briefly, the hearts were collected and preserved in 4% PFA for 24 h at room temperature, then embedded in paraffin for sectioning. The 4-μm sections were dewaxed in water and then underwent antigen retrieval in EDTA (pH 8.0) at ~98˚C for 20 min. After natural cooling, the sections were placed in PBS (pH 7.4) and washed three times with agitation (5 min each). For staining of intracellular antigens, 0.1% Triton X-100 was used as the permeabilization reagent. The sections were then incubated with 3% hydrogen peroxide solution at room temperature for 25 min in the dark, and were placed in PBS (pH 7.4) and washed three times with agitation (5 min each). Subsequently, the sections were uniformly covered with 3% BSA (cat. no. GC305010; Wuhan Servicebio Technology Co., Ltd.) and were blocked at room temperature for 30 min. The sections were incubated with primary antibodies raised against the proteins of interest at 4˚C overnight, followed by incubation with a biotin-labeled IgG secondary antibody (1:200; cat. no. GB23303; Wuhan Servicebio Technology Co., Ltd.) at room temperature for 50 min. Following 3,3'-diaminobenzidine staining and subsequent hematoxylin counterstaining, a light microscope was used to observe the expression levels of Bcl-2, Bax and caspase-3. ImageJ software (version 1.51n; National Institutes of Health) was used to analyze the average optical density values, which were calculated as the integrated density divided by the area.

Cell culture. The H9c2 rat myocardial cell line was obtained from Haixing Biotechnology Co., Ltd. The H9c2 cells were cultured in DMEM (cat. no. SH30243.FS; Cytiva), supplemented with 10% fetal bovine serum (FBS; cat. no. BC-SE-FBS01; Nanjing SenBeiJia Biological Technology Co., Ltd.) and Penicillin-Streptomycin Solution (100X; cat. no. C0222; Beyotime Institute of Biotechnology) in a humidified incubator (Shanghai Lishen Scientific Equipment Co., Ltd.) maintained at 37˚C in the presence of 5% CO_2.

Cell counting kit-8 (CCK-8) assay. H9c2 cell viability was assessed using a CCK-8 assay (Beyotime Institute of Biotechnology), following the manufacturer's instructions. Briefly, $3x10^3$ cells were plated in each well of a 96-well culture plate and exposed to various concentrations of AC (0, 20, 40,

60, 80, 100 μg/ml) for 24 h under hypoxia/reoxygenation (H/R) conditions (22,23). Subsequently, 10 μl CCK-8 solution was added to each well and incubated at 37˚C for 1.5 h. Finally, the absorbance of the samples was quantified at 450 nm using a BioTek® Synergy H1 microplate reader (Agilent Technologies, Inc.).

Establishment of the H/R cell model. H9c2 cells were divided into the Control group, the H/R group and the AC + H/R group. The cells in the AC + H/R group were pretreated with 80 μg/ml AC (dissolved in DMEM) for a duration of 24 h at 37˚C. The cells in the H/R and the AC + H/R groups were then subjected to hypoxic conditions (1% O_2) in glucose and FBS-free culture medium, whereas the cells in the Control group were untreated. After 8 h of oxygen deprivation, the H9c2 cells were reoxygenated for 12 h in normal condition as aforementioned (22,23).

Quantification of the accumulation of reactive oxygen species (ROS) in H9c2 cells. The ROS assay kit (cat. no. CA1410; Beijing Solarbio Science & Technology Co., Ltd.) was used to assess the accumulation of ROS in the H9c2 cells of each group. Briefly, the cells were incubated in DMEM lacking FBS, but containing 10 μM dichlorodihydrofluorescein diacetate (DCFH-DA), at 37˚C for 20 min. Following this incubation, the cells were washed three times with DMEM to remove any excess reagent. Subsequently, the levels of fluorescence resulting from the DCFH agent were visualized using a Leica DMI fluorescence microscope (Leica Microsystems GmbH).

Hoechst 33342 staining. Hoechst 33342 staining (cat. no. C0030; Beijing Solarbio Science & Technology Co., Ltd.) was conducted to evaluate the level of apoptosis of the H9c2 cells in each group. The H9c2 cells were seeded in 6-well plates at a density of $3x10^5$ cells per well. Cells were then incubated with 1 ml Hoechst 33342 for 5 min at room temperature, followed by washing of the wells three times with PBS. Subsequently, the fluorescence of the H9c2 cells in each group was observed under a Leica DMI 4000 fluorescence microscope (Leica Microsystems GmbH).

Western blot analysis. RIPA lysis buffer (Beyotime Institute of Biotechnology) supplemented with 1% phenylmethylsulfonyl fluoride was used to extract total protein from the cardiac tissue or H9c2 cells. The samples were incubated at 4˚C for 15 min for adequate lysis, followed by centrifugation at 15,000 x g for an additional 15 min at 4˚C. The supernatant was then collected and subjected to boiling to denature the proteins. The protein concentration of the samples was determined using a BCA assay kit (Beyotime Institute of Biotechnology). Equal amounts (20 μg) of protein were then separated by SDS-PAGE on 10-12.5% gels, followed by transfer of the proteins onto a polyvinylidene fluoride membrane. The membrane was subsequently incubated with EpiZyme™ Protein Free Rapid Blocking Buffer (cat. no. PS108P; Epizyme, Inc.) at room temperature for 15 min. Membranes were then incubated overnight with the primary antibodies of interest at 4˚C. The primary antibodies and their respective dilutions were as follows: Anti-HSP90AA1 (1:2,000 dilution; cat. no. BF0084; Affinity Biosciences), anti-PI3K (1:2,000; cat. no. BM5187; Wuhan Boster Biological Technology, Ltd.), anti-phosphorylated (p)-PI3K (1:2,000; cat. no. AF3242; Affinity Biosciences), anti-Akt (1:2,000; cat. no. AF0836; Affinity Biosciences), anti-p-Akt (1:2,000; cat. no. BM4744; Wuhan Boster Biological Technology, Ltd.), anti-GSK-3β (1:2,000; cat. no. AF5016; Affinity Biosciences), anti-p-GSK3β (1:2,000; cat. no. AF2016; Affinity Biosciences) and anti-GAPDH (1:3,000; cat. no. GB11002-100; Wuhan Servicebio Technology Co., Ltd.) Subsequently, the membrane was incubated with a horseradish peroxidase-labeled secondary antibody (1:2,000; cat. no. AS014; ABclonal Biotech Co., Ltd.). for 50 min at 37˚C. The visualization of protein bands was achieved using an ECL kit (cat. no. MA0186; Dalian Meilun Biology Technology Co., Ltd.) and the results were analyzed using a 5200 Multi gel imaging system (Tanon Science and Technology Co., Ltd.). Semi-quantification of the protein bands was performed using ImageJ software, and the protein levels were normalized against those of GAPDH, which served as the control.

Statistical analysis. Quantitative data are presented as the mean ± standard deviation. The *in vitro* experiments were repeated at least three times. For comparisons among multiple groups, one-way ANOVA was carried out, followed by Tukey's post hoc test, utilizing SPSS 27.0 software (IBM Corp.). $P<0.05$ was considered to indicate a statistically significant difference.

Results

Determination of the overlapping targets between AC and MIRI. From the database searches, a total of 2,875 genes associated with MIRI and 44 AC-associated target genes were identified. A comparison of the MIRI genes with the AC-associated targets revealed a total of 23 common genes (Fig. 2A).

Determination of the key targets of AC against MIRI. Intersection targets that were identified between AC and MIRI were inputted into the STRING database. Nodes without connections in the network diagram were removed to obtain the visualization of the PPI network (Fig. 2B). GO enrichment analysis revealed that AC may participate in various biological processes, mainly 'positive regulation of protein phosphorylation', 'positive regulation of MAP kinase activity', 'positive regulation of ERK1 and ERK2 cascade' and 'positive regulation of endothelial cell migration' (Fig. 2D). The primary cellular components (e.g. 'extracellular region', 'extracellular exosome', 'extracellular space', 'extracellular matrix' and 'perinuclear region of cytoplasm') and molecular functions (e.g. 'integrin binding', 'heparin binding', 'enzyme binding' and 'chemoattractant activity') associated with AC and MIRI are also shown in Fig. 2D. Furthermore, the KEGG enrichment analysis revealed that the overlapping genes were associated with 'Pathways in cancer', 'PI3K/Akt signaling pathway' and 'Calcium signaling pathway' (Fig. 2E).

Construction of AC-target genes/pathways-MIRI network. As shown in Fig. 2C, the therapeutic mechanism underlying how AC may ameliorate MIRI involves key targets including HSP90AA1, fibroblast growth factor 2 and IL2. Some of the implicated pathways include the PI3K/Akt

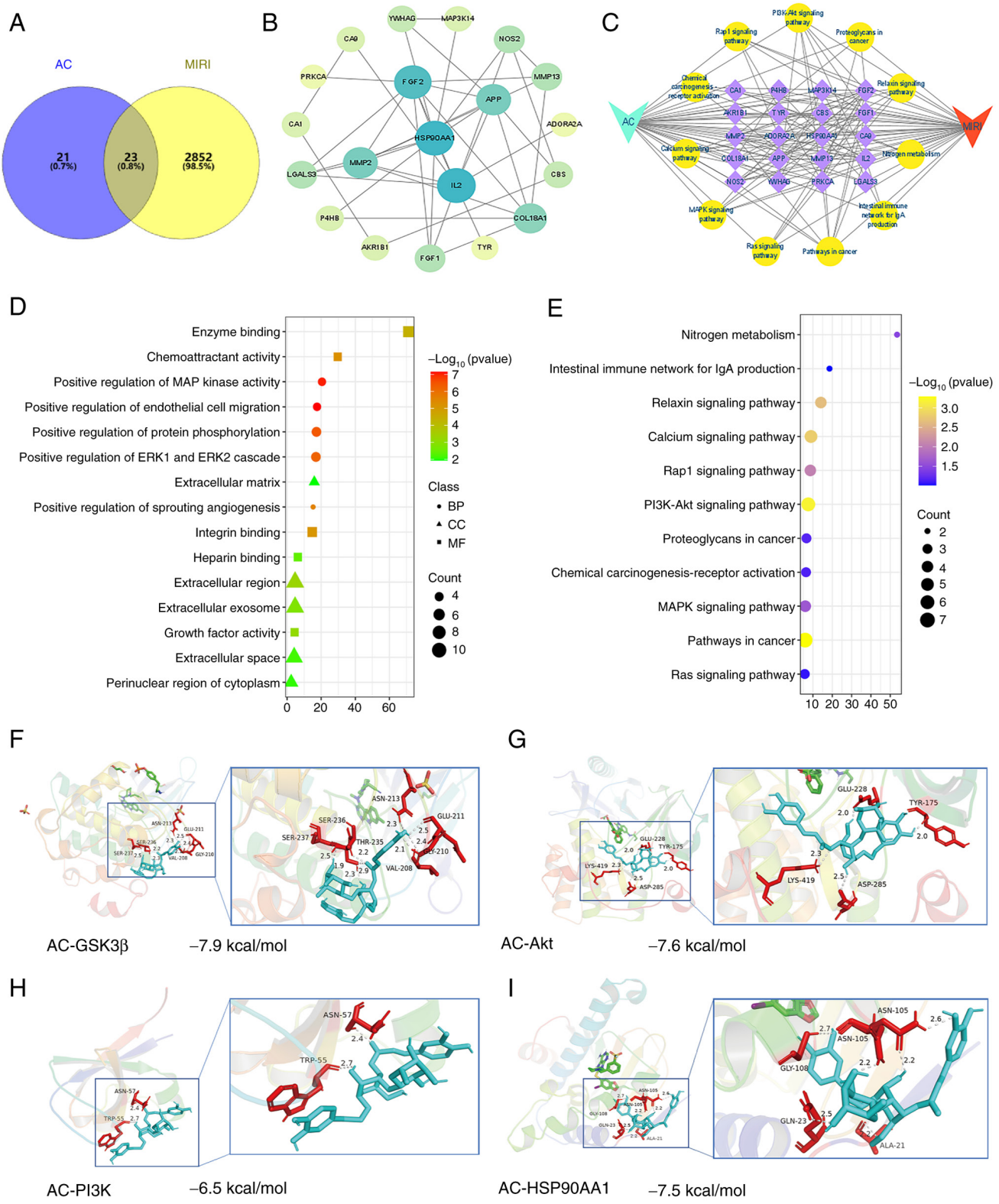

Figure 2. Network pharmacological analysis identified the key targets associated with both AC and MIRI. Molecular docking analysis confirmed the interactions of AC with the key targets. (A) A Venn diagram illustrating the targets of AC and MIRI revealed an overlap of 23 targets. (B) Visualization of the protein-protein interaction network. (C) Construction of AC-key target genes/pathways-MIRI network. (D) Results of GO enrichment analysis. (E) Results of KEGG pathway enrichment analysis. Molecular docking analyses of AC and (F) GSK-3β, (G) Akt. (H) PI3K and (I) HSP90AA1. MIRI, myocardial ischemia-reperfusion injury; AC, acteoside; BP, biological processes; CC, cellular components; MF, molecular functions; PI3K, phosphoinositide 3-kinase; HSP90AA1, heat-shock protein 90AA1; Akt, serine-threonine protein kinase; GSK-3β, glycogen synthase kinase-3β.

signaling pathway, tumor signaling pathways and the Rap1 signaling pathway. Based on the outcomes of the network pharmacological analysis, HSP90AA1 and the PI3K/Akt signaling pathway emerged as the primary targets for AC against MIRI. according to the calculation performed using Cytoscape software.

Molecular docking of AC with key target proteins. Molecular docking analysis was subsequently carried out to confirm the interactions of AC with HSP90AA1, PI3K, Akt and GSK-3β (Fig. 2F-I). The outcomes revealed that the binding energies between AC and these key proteins were all below-5.0 kcal/mol. GSK-3β exhibited the strongest binding affinity, as evidenced by the lowest (most negative) binding energy.

Establishment of the MIRI rat model using ECG monitoring. As shown in Fig. 3A, the representative ECG scans in the three experimental groups prior to thoracotomy were all normal. Notable elevations of the ST segments in rats with MIRI following LAD coronary artery occlusion were observed during the period of ischemia, when compared with the rats in the Sham group. During the reperfusion phase, the ECG for the Sham group remained normal. In comparison with the Sham group, the MIRI group exhibited a slower heart rate accompanied by persistent elevation in the ST segment. Notably, the rats in the AC + MIRI group exhibited markedly reduced ST segments and a rapid heart rate compared with those in the MIRI group.

Preconditioning with AC leads to a reduction in the MI area in rats. MI size was assessed using TTC staining. The results revealed that the MIRI experimental group had the largest MI size among the three groups. In comparison with the MIRI group, the MI size in the AC + MIRI group was significantly reduced (Fig. 3D and E). The results of TTC staining further confirmed the successful establishment of the MIRI rat model, as well as the cardioprotective effects exerted by preconditioning with AC.

Preconditioning with AC attenuates MIRI in rats. H&E staining revealed that distinct pathological hallmarks of myocardial damage had occurred in the MIRI group, including myocardial fiber fracture, cellular edema, hemorrhage and necrosis. However, these histological characteristics of myocardial structure injury were observed to be less severe in the AC + MIRI group (Fig. 3F). In addition, the establishment of MIRI led to significant myocardial injury in rats, as evidenced by the elevated serum levels of cTnI and CK-MB; however, pretreatment with AC mitigated the abnormal changes in these biochemical markers (Fig. 3B and C). Taken together, these findings corroborated the aforementioned results that preconditioning with AC may attenuate MIRI in rats.

Preconditioning with AC inhibits cardiomyocyte apoptosis in the rat model of MIRI. TUNEL staining revealed that preconditioning with AC decreased the apoptosis of cardiomyocytes triggered by MIRI (Fig. 4B and F). Subsequently, the expression levels of proteins associated with apoptosis were examined using immunohistochemical analysis (Fig. 4A, C and E). The findings demonstrated that the expression levels of Bax and caspase-3 were simultaneously suppressed, whereas those of Bcl-2 were increased by AC preconditioning, thereby confirming the inhibitory effect of AC on apoptosis during MIRI.

Preconditioning with AC alleviates H/R injury in H9c2 cells. Following the incubation of the H9c2 cells with increasing concentrations of AC (0, 50, 100, 150 and 200 μg/ml) for 24 h, cell viability was examined using a CCK-8 assay. The results suggested that, at AC concentrations of >100 μg/ml, there was a decrease in cell viability (Fig. 5A). Subsequently, the optimal concentration of AC for H9c2 cells subjected to H/R injury was assessed. The H9c2 cells were divided into the Control group, the H/R group and the AC + H/R group. Prior to the establishment of the H/R injury cell model, the H9c2 cells in the AC + H/R group were exposed to increasing concentrations of AC (20, 40, 60, 80 and 100 μg/ml) for a duration of 24 h. Based on the results of the CCK-8 assay, a concentration of 80 μg/ml AC was selected for further experiments (Fig. 5B). A significant reduction in the viability of the H9c2 cells was observed following H/R intervention when compared with the Control group. The application of 80 μg/ml AC resulted in significant amelioration of cell viability when compared with the H/R group (Fig. 5C). Furthermore, compared with in the Control group, detrimental morphological changes of the H9c2 cells, characterized by a loss of membrane integrity and shrinkage were observed in the H/R group, this was prevented with AC preconditioning (Fig. 5D). Finally, Hoechst 33342 staining demonstrated that H/R injury led to an increase in the apoptotic rate of the H9c2 cells when compared with the Control group, whereas preconditioning with AC attenuated the apoptotic response in H9c2 cells subjected to the H/R condition (Fig. 6A).

Preconditioning with AC suppresses oxidative stress during the establishment of MIRI in vivo and in vitro. To evaluate the antioxidant potential of AC, the levels of SOD and MDA were detected within the myocardial tissues, as well as ROS levels in the H9c2 cells. The results revealed that rats subjected to MIRI displayed increased MDA activity and diminished SOD levels, when compared with the Sham group (Fig. 3G and H). In addition, there was a marked elevation in the intracellular ROS concentration in the H/R group compared with the Control group (Fig. 5E). Notably, preconditioning with AC mitigated this increase.

Preconditioning with AC has a cardioprotective effect against MIRI through modulation of the expression levels of HSP90AA1, PI3K, Akt and GSK-3β. Western blot analysis was used to detect the expression levels of key target proteins associated with AC and MIRI *in vivo* and *in vitro*. As shown in Fig. 4G-K, there was an upregulation in the expression of HSP90AA1 in myocardial tissue in both the MIRI and the AC + MIRI groups when compared with the Sham group. Notably, the AC + MIRI group exhibited a more pronounced increase in the expression of HSP90AA1 when compared with the MIRI group. Furthermore, the AC + MIRI group demonstrated increased expression of the phosphorylated forms of the proteins of interest, p-PI3K, p-Akt and p-GSK3β, compared with both the MIRI and Sham groups. These outcomes are consistent with the findings in the MIRI rat model (Fig. 6B-F).

Discussion

The risk of MIRI increases with longer durations of ischemia and more severe ischemic conditions (24). Ischemic

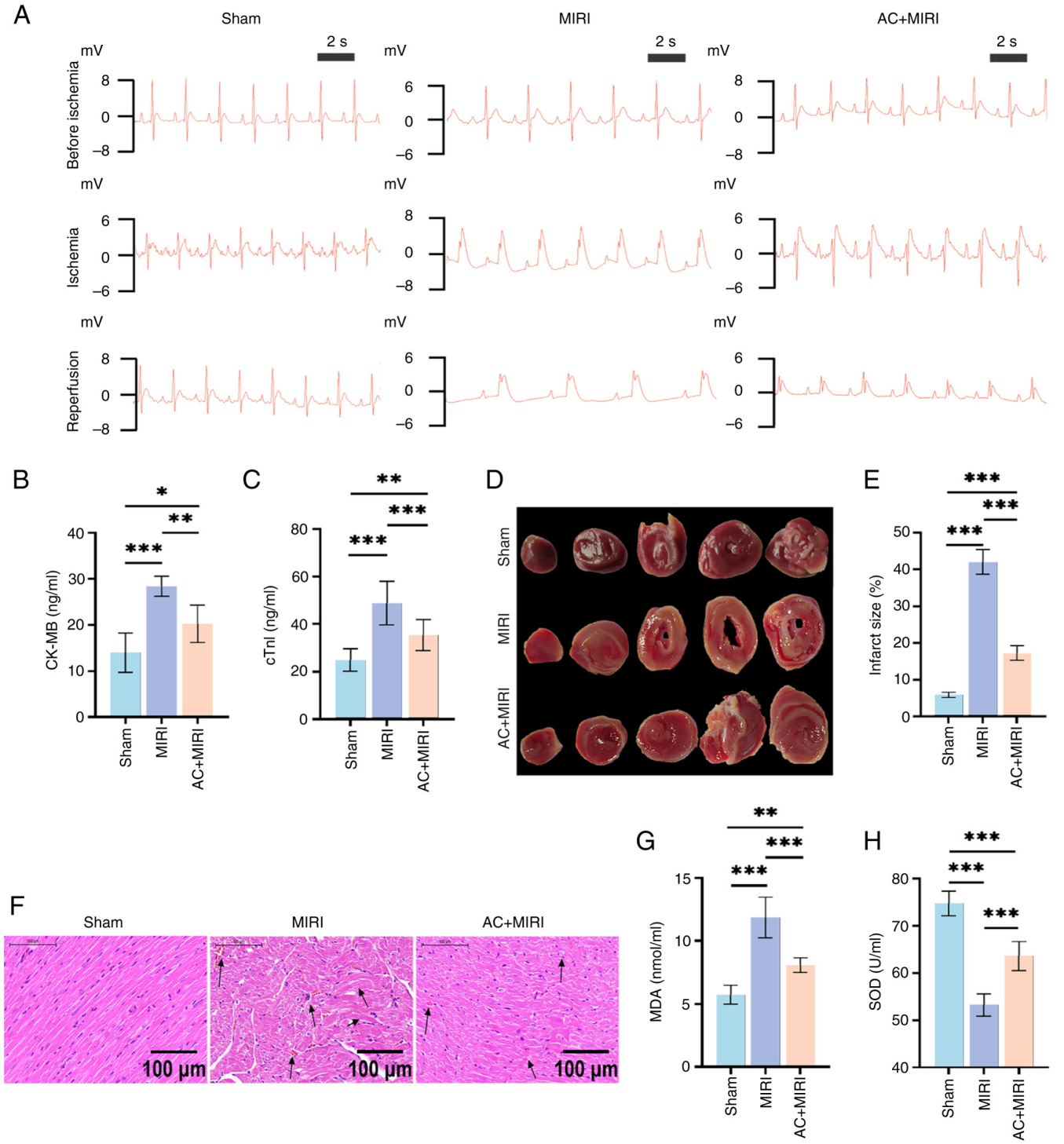

Figure 3. Preconditioning with AC attenuates myocardial damage caused by MIRI and inhibits oxidative stress in rats. (A) Representative electrocardiograms of rats subjected to either Sham, MIRI or AC + MIRI treatment before ischemia, during ischemia and during reperfusion (n=15). Quantification of serum (B) CK-MB (n=6) and (C) cTnI levels in rats subjected to either Sham, MIRI or AC + MIRI treatment (n=10). (D) Representative images of 2,3,5-triphenyltetrazolium chloride-stained heart sections of rats subjected to either Sham, MIRI or AC + MIRI treatment (n=5). (E) Quantification of myocardial infarct size in rats subjected to either Sham, MIRI or AC + MIRI treatment. (F) Representative images of hematoxylin and eosin-stained heart section in rats subjected to either Sham, MIRI or AC + MIRI treatment (n=5). Quantification of serum (G) MDA and (H) SOD levels in rats subjected to either Sham, MIRI or AC + MIRI treatment (n=6). Data are presented as the mean ± standard deviation. *P<0.05; **P<0.01; ***P<0.001. MIRI, myocardial ischemia-reperfusion injury; ACI, acteoside; CK-MB, creatine kinase MB isoenzyme; cTn1, cardiac troponin I; MDA, malondialdehyde; SOD, superoxide dismutase.

preconditioning, ischemic postconditioning, remote ischemic conditioning, cell therapy and pharmacological interventions have been developed to prevent or alleviate MIRI, and to improve patient outcomes (25,26). The present study revealed that AC preconditioning may be a promising therapeutic method for MIRI. The main findings were, i) AC attenuated cardiac injury, as evidenced by a reduced infarct area, altered serum levels of biochemical markers, reduced pathological damage of myocardial tissue and improved H9c2 cell viability; ii) AC inhibited the apoptosis of cardiomyocytes and oxidative

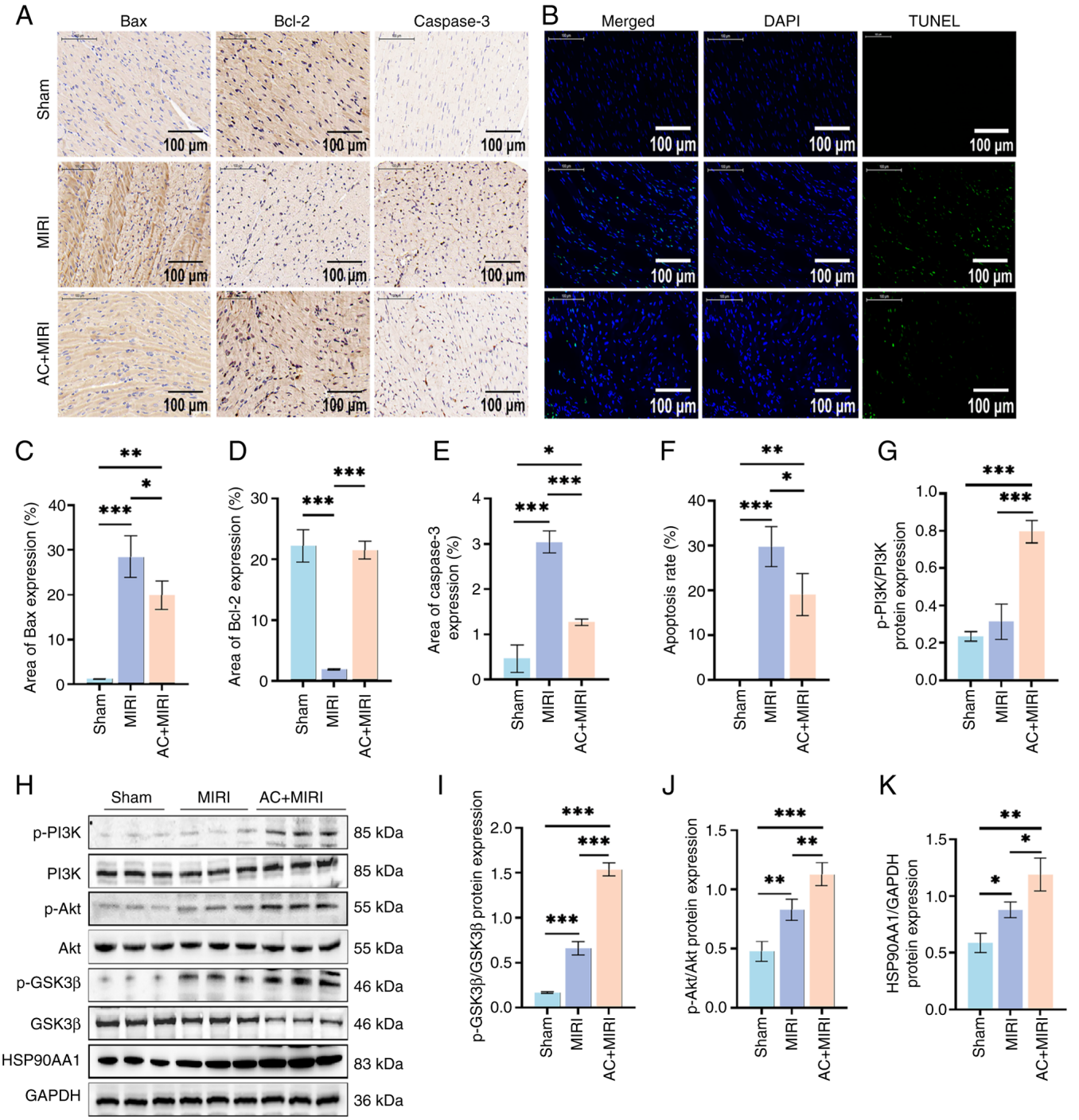

Figure 4. Preconditioning with AC suppresses cardiomyocyte apoptosis and regulates the expression of key target proteins in rats during MIRI (n=5). (A) Representative immunohistochemistry sections of Bax, Bcl-2 and caspase-3 expression in myocardial tissue from rats subjected to either Sham, MIRI or AC + MIRI treatment. (B) Representative TUNEL assay sections of myocardial tissue from rats subjected to either Sham, MIRI or AC + MIRI treatment. Quantification of (C) Bax, (D) Bcl-2 and (E) caspase-3 expression in myocardial tissue of rats subjected to either Sham, MIRI or AC + MIRI treatment. (F) Quantification of cardiomyocyte apoptosis in rats subjected to either Sham, MIRI or AC + MIRI treatment. (H) Western blot analysis detected the levels of HSP90AA1 and phosphorylation of PI3K, Akt and GSK3β in the myocardial tissue of rats subjected to either Sham, MIRI or AC + MIRI treatment. Semi-quantification of (G) p-PI3K, (I) p-GSK-3β, (J) p-Akt and (K) HSP90AA1 in rats subjected to either Sham, MIRI or AC + MIRI treatment. Data are presented as the mean ± standard deviation. *P<0.05, **P<0.01, ***P<0.001. MIRI, myocardial ischemia-reperfusion injury; AC, acteoside; TUNEL, terminal deoxynucleotidyl transferase mediated dUTP nick end labeling; p-, phosphorylated; PI3K, phosphoinositide 3-kinase; HSP90AA1, heat-shock protein 90AA1; Akt, serine-threonine protein kinase; GSK-3β, glycogen synthase kinase-3β.

stress during MIRI; and iii) AC both increased the expression levels of HSP90AA1, and regulated the expression and activation of key target proteins, including PI3K, Akt and GSK-3β.

Damage due to oxidative stress arises when there is an imbalance between the production of ROS and the ability of the body to neutralize or eliminate ROS through antioxidant mechanisms (27). Oxidative stress is considered to be a key initiating factor in the pathogenesis of injuries, such as those that arise from MIRI. Numerous studies have suggested that the suppression of oxidative stress may serve as an effective

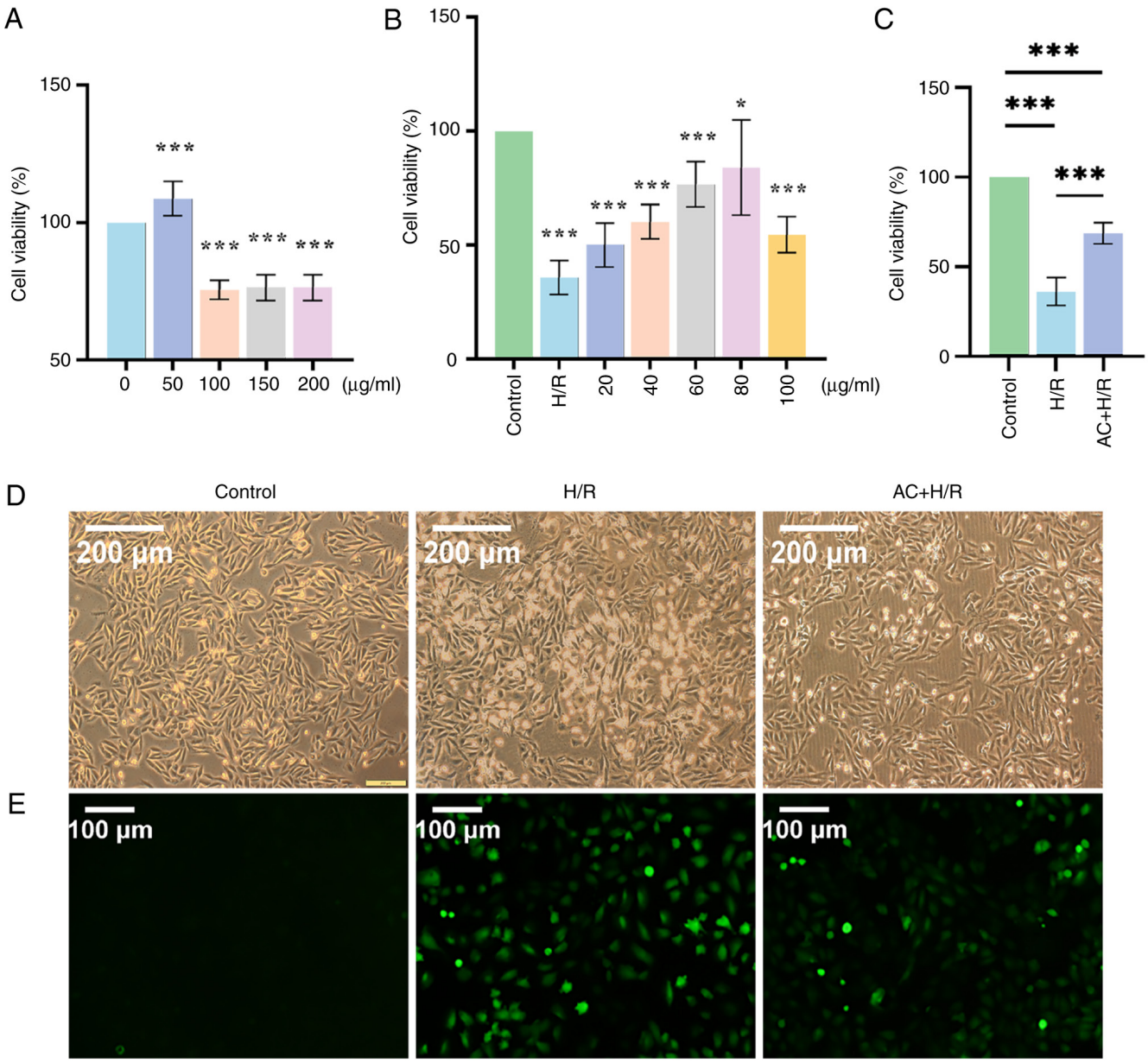

Figure 5. Preconditioning with AC improves cell viability and morphological alterations, while it mitigates oxidative stress in H9c2 cells against MIRI. (A) CCK-8 assay was utilized to assess the impact of various concentrations of AC on the viability of H9c2 cells. (B) CCK-8 assay was used to determine the final concentration of AC (80 μg/ml) used to treat the H9c2 cells. (C) CCK-8 assay showed the H9c2 cells exposed to H/R had reduced cell viability, which was prevented by preconditioning H9c2 cells with AC. (D) Representative microscopic images showed the morphological changes of H9c2 cells subjected to H/R and AC + H/R compared with control cells (magnification x200; scale bar, 200 μm). (E) Representative microscopic images showed the intracellular reactive oxygen species levels of H9c2 cells subjected to H/R and AC + H/R compared with control cells (magnification x200; scale bar, 100 μm). Data are presented as the mean ± standard deviation. *P<0.05 and ***P<0.001 vs. the Control group or as indicated. H/R, hypoxia/reoxygenation; AC, acteoside; CCK-8, Cell Counting Kit-8.

strategy to alleviate MIRI (28,29). AC demonstrates protection against oxidative stress triggered by IRI, as evidenced by a reduction in the levels of ROS and MDA, and increased production of SOD and catalase (CAT) (30,31). Consistent with these findings, the present study revealed that H9c2 cells subjected to H/R injury exhibited excessive ROS generation, and in a rat model of MIRI, serum MDA levels were elevated and SOD levels were reduced. However, pretreatment with AC caused a significant increase in the antioxidant capacity of cardiomyocytes, effectively alleviating the harmful consequences of ROS. By eliminating ROS and enhancing the antioxidant defenses, AC reduced oxidative stress, thereby mitigating the initial insult of MIRI.

Studies have shown that the apoptosis of cardiomyocytes contributes to determining the extent of myocardial tissue damage and subsequent cardiac dysfunction (32,33). Cardiomyocyte apoptosis may be triggered by oxidative stress, calcium overload, inflammation and energy depletion during MIRI. Several signaling pathways have been shown to be associated with mediating cardiomyocyte apoptosis. The mitochondrial pathway, which is mediated by the Bcl-2 family of proteins and caspase cascade activation, is particularly important. MIRI causes an impairment of mitochondrial function, resulting in the release of cytochrome *c* and other apoptotic factors into the cytosol, thereby activating caspase cascades that ultimately lead to cardiomyocyte apoptosis. A recent study demonstrated the protective role of AC

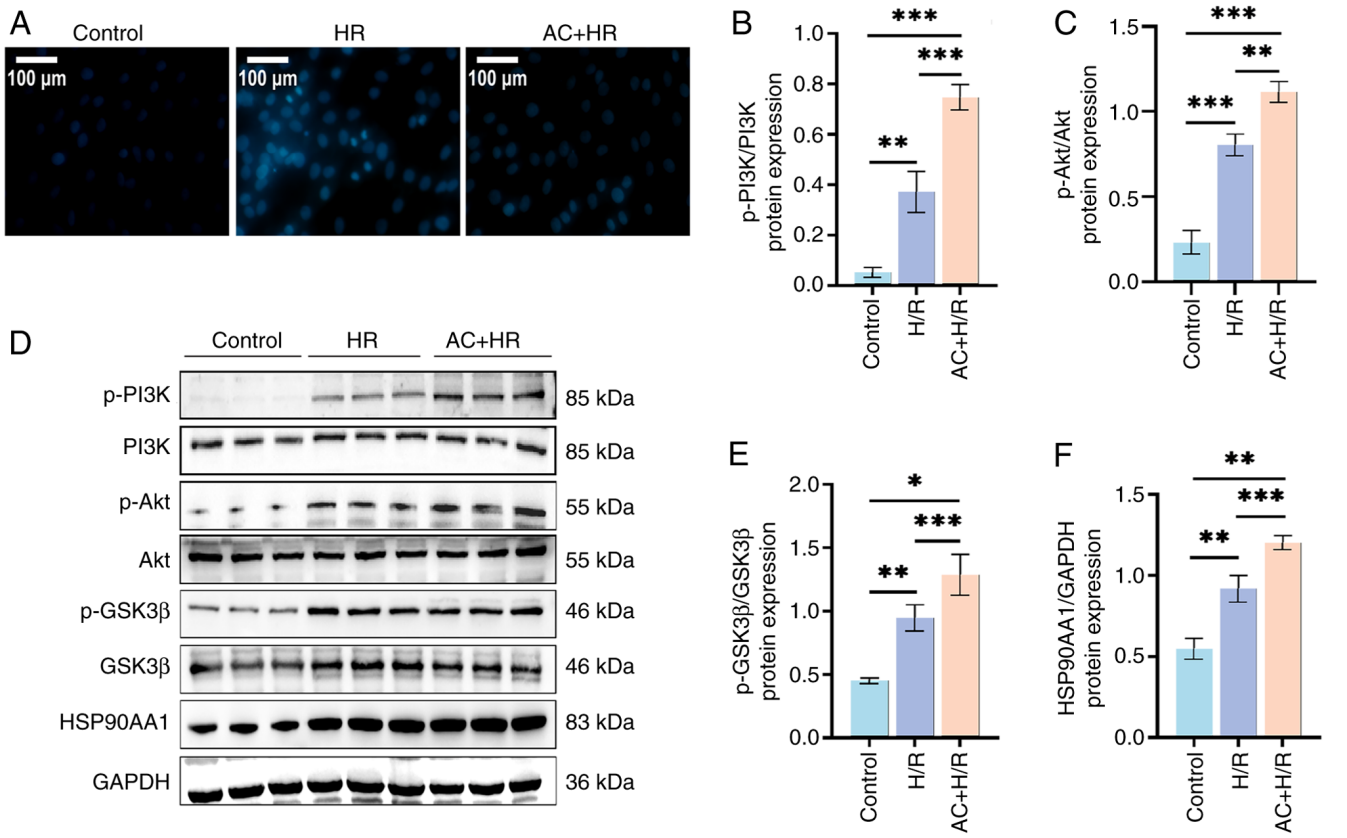

Figure 6. Preconditioning with AC suppresses apoptosis and regulates the expression of key target proteins in H9c2 cells subjected to H/R. (A) Representative microscopic images of Hoechst 33342 staining shows the apoptosis of control H9c2 cells, and H9c2 cells subjected to H/R and AC + H/R (magnification x200; scale bar, 100 μm). (B) Western blot analysis detected the expression levels of HSP90AA1, and the levels of p-PI3K, p-Akt and p-GSK-3β in control H9c2 cells, and H9c2 cells subjected to H/R and AC + H/R. Semi-quantification of (C) p-PI3K, (D) p-Akt, (E) p-GSK-3β and (F) HSP90AA1 in the H9c2 cells of three groups. Data are presented as the mean ± standard deviation. *P<0.05; **P<0.01; ***P<0.001. H/R, hypoxia/reoxygenation; AC, acteoside; p-, phosphorylated; PI3K, phosphoinositide 3-kinase; HSP90AA1, heat-shock protein 90AA1; Akt, serine-threonine protein kinase; GSK-3β, glycogen synthase kinase-3β.

against sepsis-triggered cardiomyopathy, which was achieved through decreasing the levels of oxidative stress, inflammation and apoptosis, while concurrently promoting mitochondrial biogenesis (34). Based on these insights, the anti-apoptotic potential of AC in MIRI was investigated in the present study. As predicted, the results of the TUNEL staining, Hoechst 33342 staining and immunohistochemical analysis suggested that preconditioning with AC may prevent MIRI-induced cardiomyocyte apoptosis by upregulating the expression of Bcl-2, and downregulating the expression of Bax and caspase-3. Furthermore, previous studies have highlighted the capacity of AC to influence other apoptotic signaling pathways, including the Akt/GSK-3β and nuclear factor erythroid 2-related factor 2/antioxidant response element pathways, which further reinforce its anti-apoptotic function (35,36).

Network pharmacological analysis, an emerging interdisciplinary field, has been shown to have an important role in advancing drug discovery and development, as well as in elucidating the complex mechanisms underlying therapeutic interventions (37). Therefore, network pharmacological analysis was used in the present study to screen the possible key targets that may participate in the mechanism underlying the therapeutic action of AC against MIRI and furthermore, molecular docking was used to predict the binding orientation of AC to target proteins at the molecular level. These analyses revealed that the screened key targets, HSP90AA1, PI3K, Akt and GSK-3β, all exhibited good binding with AC. The expression levels of HSP90AA1, PI3K and Akt, as well as GSK-3β, the downstream signaling molecule of Akt, were also assessed in both H9c2 cells and the myocardial tissue of rats. Moreover, changes in the expression levels of p-PI3K, p-Akt and p-GSK-3β were assessed. Preconditioning with AC was found to increase both the expression levels of HSP90AA1, and the phosphorylated forms of PI3K, Akt and GSK-3β.

As has been demonstrated previously, HSP90AA1 acts as an important molecular chaperone, facilitating the accurate folding and stabilization of several client proteins. This function is important in terms of preserving the structural integrity and functional capabilities of cardiomyocytes, both during and after ischemia and reperfusion events (12,13). By preserving the function of client proteins involved in cell survival and repair, HSP90AA1 may contribute to the cardioprotective effects of AC observed during MIRI, including the regulation of signaling pathways involved in cell stress responses, inflammation and repair (38). The possible downstream signals of HSP90AA1 during MIRI are autophagy-related genes, MAPK, NF-κB and hypoxia inducible factor-1α/BCL2/BNIP3, amongst others (39,40). A previous study suggested that microRNA-1 (miR-1) has a regulatory role in MIRI and HSP90AA1 has been identified as a novel target gene of miR-1. The downregulation of miR-1 post-ischemia-reperfusion has been reported to result in an increase in the expression of HSP90AA1, which may

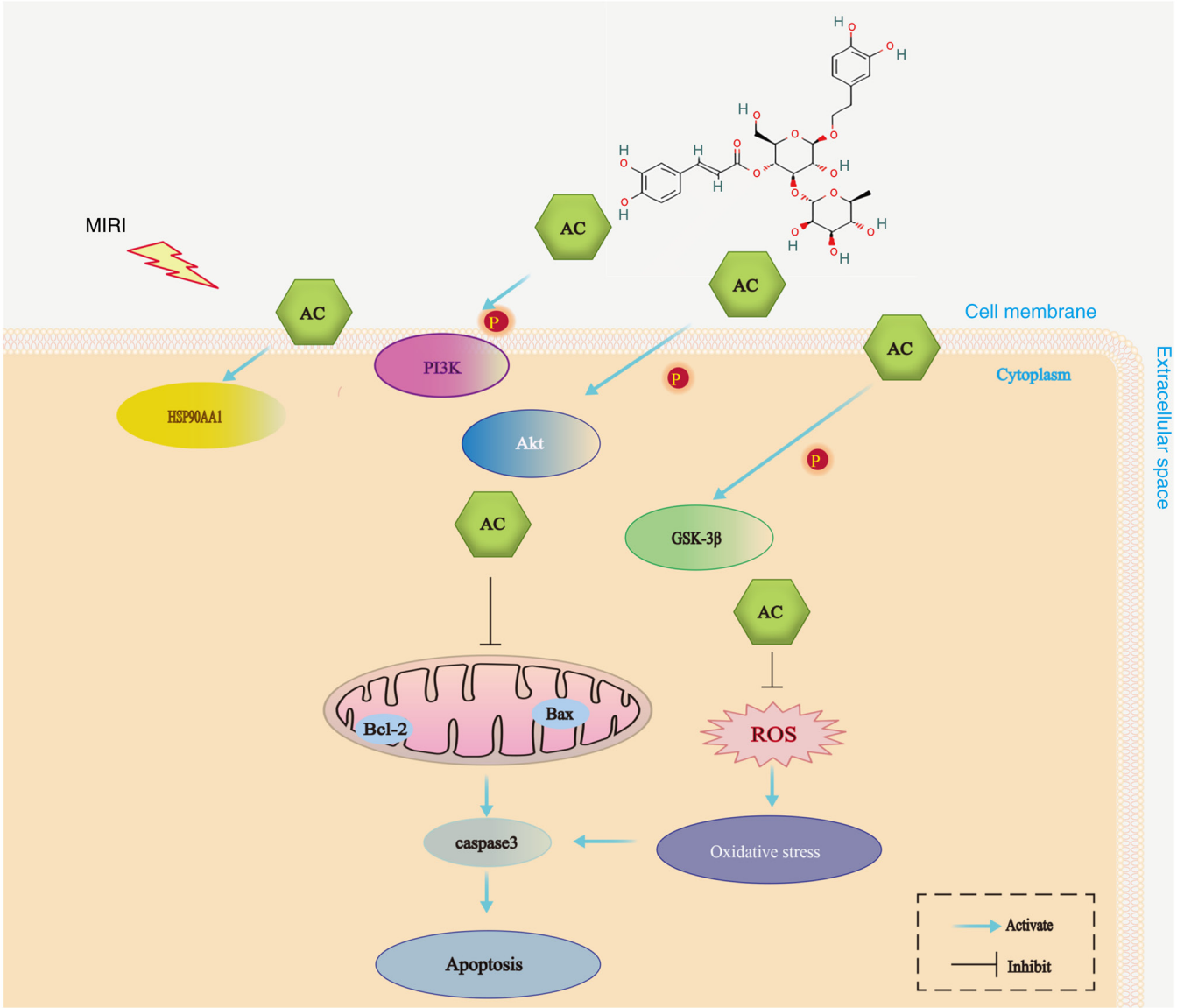

Figure 7. A schematic summary of the possible protective mechanism of AC against MIRI: AC inhibited the apoptosis of myocardial cells and oxidative stress. AC also regulated the expression and activation of key target proteins, including HSP90AA1, PI3K, Akt and GSK-3β. ROS, reactive oxygen species; AC, acteoside; PI3K, phosphoinositide 3-kinase; HSP90AA1, heat-shock protein 90AA1; Akt, serine-threonine protein kinase; GSK-3β, glycogen synthase kinase-3β; MIRI, myocardial ischemia-reperfusion injury.

be associated with the recovery of cardiomyocytes (41). HSP90AA1 has also been shown to attenuate apoptosis in neonatal rat ventricular cells subjected to oxygen-glucose deprivation, a model of ischemia (41). Considering its role in protecting cardiomyocytes from IRI, HSP90AA1 may represent a potential therapeutic target for the treatment of MI and other associated cardiovascular diseases.

The PI3K/Akt signaling pathway is an important signaling cascade that regulates a range of cellular functions, including cell survival, proliferation and metabolism (42). The importance of the PI3K/Akt pathway in protection from ischemia-reperfusion damage has been demonstrated by a number of studies (43,44). PI3K is a lipid kinase that becomes activated in response to various extracellular stimuli. Upon activation, PI3K converts phosphatidylinositol 4,5-bisphosphate into phosphatidylinositol 3,4,5-trisphosphate, which acts as a second messenger to recruit Akt to the plasma membrane, where Akt becomes phosphorylated and activated by phosphoinositide-dependent kinase 1. Activated Akt subsequently proceeds to phosphorylate downstream targets, such as GSK-3β, a downstream target of Akt that is inactivated by Akt-mediated phosphorylation and is involved in multiple cellular processes, including glycogen metabolism, cell survival and apoptosis (45,46). Apoptosis and oxidative stress are contributors to MIRI, and previous studies have shown that the activation of Akt not only inhibits the apoptosis-promoting proteins Bad and caspase-9 to block the intrinsic and extrinsic apoptotic pathways, but it also promotes the expression of antioxidant enzymes, such as SOD, CAT and glutathione peroxidase (47,48). According to these studies and the findings of the present study, it may be hypothesized that AC prevents oxidative damage and apoptosis by regulating the expression levels and the function of HSP90AA1, PI3K, Akt and GSK-3β during MIRI.

The interplay between HSP90AA1 and the PI3K/Akt signaling pathway in MIRI is multifaceted. HSP90AA1 has been shown to interact directly with and stabilize key components of the PI3K/Akt pathway, including Akt itself and upstream activators (49). This interaction ensures the sustained activation of the PI3K/Akt pathway, which is key for cardioprotection during ischemia and reperfusion. HSP90AA1 may also regulate the PI3K/Akt pathway indirectly by modulating the expression or activity of other proteins that influence this signaling cascade. HSP90AA1 has been shown to regulate other cardioprotective pathways, such as those involving NF-κB and ERK, which can crosstalk with the PI3K/Akt pathway to further enhance cell survival (50,51).

In conclusion, the present study suggested that the cardioprotective effects of AC preconditioning on MIRI were achieved through a complex mechanism that includes attenuation of oxidative stress and the apoptosis of cardiomyocytes, which thereby modulates the function of HSP90AA1 and the PI3K/Akt signaling pathway (Fig. 7). These results have emphasized the therapeutic potential of AC as a novel agent for the prevention and treatment of MIRI. However, the present study is limited by the fact that the precise mechanism through which HSP90AA1 engages with and influences the PI3K/Akt signaling pathway, as well as the processes of oxidative stress and apoptosis, remains incompletely understood. Furthermore, the interaction between AC and HSP90AA1, PI3K, Akt and GSK-3β needs experimental confirmation. Therefore, future studies will focus on elucidating the detailed interactions among these key proteins and the intervention of AC on MIRI, with the aim of providing novel evidence in support of the clinical application of AC. Subsequent *in vivo* experiments, will utilize the co-immunoprecipitation (IP) technique to confirm the interactions among these key proteins. Additionally, IP experiments will be conducted to investigate the interactions between AC and these key proteins. *In vitro* experiments will also be carried out using LY294002, a specific inhibitor of PI3K, to determine the mechanism of action of AC in H9c2 cells.

Acknowledgements

Not applicable.

Funding

This present study was supported by the Natural Science Foundation of Heilongjiang Province (grant no. LH2022H091); the Open Project of Key Laboratory of Myocardial Ischemia, Ministry of Education (grant no. KF202116); the Dongji academic team of Jiamusi University (grant no. DJXSTD202409); and the Team Project of Fundamentals and Clinical Application about Cardiovascular Disease in the First Affiliated Hospital of Jiamusi University (grant no. 202301).

Availability of data and materials

The data generated in the present study may be requested from the corresponding author.

Authors' contributions

LJ, HY and GY contributed towards the experimental design. JL, YG, YY, QX and HC carried out the experiments. HC, JL and YG analyzed the data, and LJ, JL, YG, YY, QX, HC, HY and GY wrote the manuscript. All authors read and approved the final manuscript. JL and HY confirm the authenticity of all the raw data.

Ethics approval and consent to participate

The experimental procedure for the care and use of laboratory animals in the present study was approved by the Biology and Animal Ethical Committee of the Basic Medical College, Jiamusi University (approval no. JDJCYXY-2024-0021).

Patient consent for publication

Not applicable.

Competing interests

The authors declare they have no competing interests.

References

1. Su Y, Zhu C, Wang B, Zheng H, McAlister V, Lacefield JC, Quan D, Mele T, Greasley A, Liu K and Zheng X: Circular RNA Foxo3 in cardiac ischemia-reperfusion injury in heart transplantation: A new regulator and target. Am J Transplant 21: 2992-3004, 2021.
2. Xiang Q, Yi X, Zhu XH, Wei X and Jiang DS: Regulated cell death in myocardial ischemia-reperfusion injury. Trends Endocrinol Metab 35: 219-234, 2024.
3. Jo W, Kang KK, Chae S and Son WC: Metformin Alleviates left ventricular diastolic dysfunction in a rat myocardial ischemia reperfusion injury model. Int J Mol Sci 21: 1489, 2020.
4. Doulamis IP and McCully JD: Mitochondrial Transplantation for Ischemia Reperfusion Injury. Mitochondrial Medicine: Volume 3: Manipulating Mitochondria and Disease-Specific Approaches. Springer, Heidelberg, pp15-37, 2021.
5. Méndez-Valdés G, Pérez-Carreño V, Bragato MC, Hundahl M, Chichiarelli S, Saso L and Rodrigo R: Cardioprotective mechanisms against reperfusion injury in acute myocardial infarction: Targeting angiotensin II receptors. Biomedicines 11: 17, 2022.
6. Fuji Y, Uchida K, Akashi T, Ohtsuki T, Matsufuji H and Hirai MY: Molecular identification of UDP-sugar-dependent glycosyltransferase and acyltransferase involved in the phenylethanoid glycoside biosynthesis induced by methyl jasmonate in sesamum indicum L. Plant Cell Physiol 64: 716-728, 2023.
7. Cardinali A, Pati S, Minervini F, D'Antuono I, Linsalata V and Lattanzio V: Verbascoside, isoverbascoside, and their derivatives recovered from olive mill wastewater as possible food antioxidants. J Agric Food Chem 60: 1822-1829, 2012.
8. Khan RA, Hossain R, Roy P, Jain D, Saikat ASM, Shuvo APR, Akram M, Elbossaty WF, Khan IN, Painuli S, *et al*: Anticancer effects of acteoside: Mechanistic insights and therapeutic status. Eur J Pharmacol 916: 174699, 2022.
9. Xiao Y, Ren Q and Wu L: The pharmacokinetic property and pharmacological activity of acteoside: A review. Biomed Pharmacother 153: 113296, 2022.
10. Cheng XF, He ST, Zhong GQ, Meng JJ, Wang M, Bi Q and Tu RH: Exosomal HSP90 induced by remote ischemic preconditioning alleviates myocardial ischemia/reperfusion injury by inhibiting complement activation and inflammation. BMC Cardiovasc Disord 23: 58, 2023.
11. Byun JK, Lee SH, Moon EJ, Park MH, Jang H, Weitzel DH, Kim HH, Basnet N, Kwon DY, Lee CT, *et al*: Manassantin A inhibits tumour growth under hypoxia through the activation of chaperone-mediated autophagy by modulating Hsp90 activity. Br J Cancer 128: 1491-1502, 2023.

12. Zuehlke AD, Beebe K, Neckers L and Prince T: Regulation and function of the human HSP90AA1 gene. Gene 570: 8-16, 2015.
13. Sain A, Khamrai D, Kandasamy T and Naskar D: Apigenin exerts anti-cancer effects in colon cancer by targeting HSP90AA1. J Biomol Struct Dyn: 1-13, 2023 (Epub ahead of print).
14. Syed Abd Halim SA, Abd Rashid N, Woon CK and Abdul Jalil NA: Natural products targeting PI3K/AKT in myocardial ischemic reperfusion injury: A scoping review. Pharmaceuticals (Basel) 16: 739, 2023.
15. Korshunova AY, Blagonravov ML, Neborak EV, Syatkin SP, Sklifasovskaya AP, Semyatov SM and Agostinelli E: BCL2-regulated apoptotic process in myocardial ischemia-reperfusion injury (Review). Int J Mol Med 47: 23-36, 2021.
16. Wang D, Zhang X, Li D, Hao W, Meng F, Wang B, Han J and Zheng Q: Kaempferide protects against myocardial ischemia/reperfusion injury through activation of the PI3K/Akt/GSK-3β pathway. Mediators Inflamm 2017: 5278218, 2017.
17. Wu B, Cao Y, Meng M, Jiang Y, Tao H, Zhang Y, Huang C and Li R: Gabapentin alleviates myocardial ischemia-reperfusion injury by increasing the protein expression of $GABA_AR\delta$. Eur J Pharmacol 944: 175585, 2023.
18. Boovarahan SR and Kurian GA: Preconditioning the rat heart with 5-azacytidine attenuates myocardial ischemia/reperfusion injury via PI3K/GSK3β and mitochondrial K^{ATP} signaling axis. J Biochem Mol Toxicol 35: e22911, 2021.
19. National Research Council. Committee for the Update of the Guide for the Care and Use of Laboratory Animals. Guide for the care and use of laboratory animals. The National Academies Collection: Reports funded by National Institutes of Health. 8th edition. National Academies Press, Washington, DC, 2011.
20. Xu M, Li X and Song L: Baicalin regulates macrophages polarization and alleviates myocardial ischaemia/reperfusion injury via inhibiting JAK/STAT pathway. Pharm Biol 58: 655-663, 2020.
21. Pang D and Laferriere C: Review of intraperitoneal injection of sodium pentobartital as a method of euthanasia in laboratory rodents. J Am Assoc Lab Anim Sci 59: 346, 2020.
22. Han RH, Huang HM, Han H, Chen H, Zeng F, Xie X, Liu DY, Cai Y, Zhang LQ, Liu X, *et al*: Propofol postconditioning ameliorates hypoxia/reoxygenation induced H9c2 cell apoptosis and autophagy via upregulating forkhead transcription factors under hyperglycemia. Mil Med Res 8: 58, 2021.
23. Ding S, Duanmu X, Xu L, Zhu L and Wu Z: Ozone pretreatment alleviates ischemiareperfusion injury-induced myocardial ferroptosis by activating the Nrf2/Slc7a11/Gpx4 axis. Biomed Pharmacother 165: 115185, 2023.
24. Meng XM, Yuan JH, Zhou ZF, Feng QP and Zhu BM: Evaluation of time-dependent phenotypes of myocardial ischemia-reperfusion in mice. Aging (Albany NY) 15: 10627-10639, 2023.
25. Sánchez-Hernández CD, Torres-Alarcón LA, González-Cortés A and Peón AN: Ischemia/reperfusion injury: Pathophysiology, current clinical management, and potential preventive approaches. Mediators Inflamm 2020: 8405370, 2020.
26. Ferdinandy P, Andreadou I, Baxter GF, Bøtker HE, Davidson SM, Dobrev D, Gersh BJ, Heusch G, Lecour S, Ruiz-Meana M, *et al*: Interaction of cardiovascular nonmodifiable risk factors, comorbidities and comedications with ischemia/reperfusion injury and cardioprotection by pharmacological treatments and ischemic conditioning. Pharmacol Rev 75: 159-216, 2023.
27. Bugger H and Pfeil K: Mitochondrial ROS in myocardial ischemia reperfusion and remodeling. Biochim Biophys Acta Mol Basis Dis 1866: 165768, 2020.
28. Orellana-Urzúa S, Rojas I, Líbano L and Rodrigo R: Pathophysiology of ischemic stroke: Role of oxidative stress. Curr Pharm Des 26: 4246-4260, 2020.
29. Dambrova M, Zuurbier CJ, Borutaite V, Liepinsh E and Makrecka-Kuka M: Energy substrate metabolism and mitochondrial oxidative stress in cardiac ischemia/reperfusion injury. Free Radic Biol Med 165: 24-37, 2021.
30. Xia D, Zhang Z and Zhao Y: Acteoside attenuates oxidative stress and neuronal apoptosis in rats with focal cerebral ischemia-reperfusion injury. Biol Pharm Bull 41: 1645-1651, 2018.
31. Değer AN, Özyiğit F, Koçak FE, Bayhan Z, Zeren S, Arık Ö and Değer H: Corrective effect of verbascoside on histomorphological differences and oxidative stress in colon mucosa of rats in which colon ischemia-reperfusion injury was induced. urk J Gastroenterol 32: 548-549, 2021.
32. Ye HK, Zhang HH and Tan ZM: MiR-328 inhibits cell apoptosis and improves cardiac function in rats with myocardial ischemia-reperfusion injury through MEK-ERK signaling pathway. Eur Rev Med Pharmacol Sci 24: 3315-3321, 2020.
33. Toldo S, Mauro AG, Cutter Z and Abbate A: Inflammasome, pyroptosis, and cytokines in myocardial ischemia-reperfusion injury. Am J Physiol Heart Circ Physiol 315: H1553-H1568, 2018.
34. Zhu X, Sun M, Guo H, Lu G, Gu J, Zhang L, Shi L, Gao J, Zhang D, Wang W, *et al*: Verbascoside protects from LPS-induced septic cardiomyopathy via alleviating cardiac inflammation, oxidative stress and regulating mitochondrial dynamics. Ecotoxicol Environ Saf 233: 113327, 2022.
35. Li X, Liu Z, He Z, Wang X, Li R, Wang J, Ma G, Zhang P and Ma C: Acteoside protects podocyte against apoptosis through regulating AKT/GSK-3β signaling pathway in db/db mice. BMC Endocr Disord 23: 230, 2023.
36. Li M, Xu T, Zhou F, Wang M, Song H, Xiao X and Lu B: Neuroprotective effects of four phenylethanoid glycosides on H_2O_2-induced apoptosis on PC12 cells via the Nrf2/ARE Pathway. Int J Mol Sci 19: 1135, 2018.
37. Noor F, Asif M, Ashfaq UA, Qasim M and Tahir Ul Qamar M: Machine learning for synergistic network pharmacology: A comprehensive overview. Brief Bioinform 24: bbad120, 2023.
38. Zheng Y, Chen S, Yang Y, Li X, Wu J, Liu J, Wang Y, Qi X, Wang Y, Liu Z, *et al*: Uncovering the molecular mechanisms of Ilex pubescens against myocardial ischemia-reperfusion injury using network pharmacology analysis and experimental pharmacology. J Ethnopharmacol 282: 114611, 2022.
39. Singh KK, Yanagawa B, Quan A, Wang R, Garg A, Khan R, Pan Y, Wheatcroft MD, Lovren F, Teoh H and Verma S: Autophagy gene fingerprint in human ischemia and reperfusion. J Thorac Cardiovasc Surg 147: 1065-1072.e1, 2014.
40. Chen Z, Liu T, Yuan H, Sun H, Liu S, Zhang S, Liu L, Jiang S, Tang Y and Liu Z: Bioinformatics integration reveals key genes associated with mitophagy in myocardial ischemia-reperfusion injury. BMC Cardiovasc Disord 24: 183, 2024.
41. Zhu WS, Guo W, Zhu JN, Tang CM, Fu YH, Lin QX, Tan N and Shan ZX: Hsp90aa1: A novel target gene of miR-1 in cardiac ischemia/reperfusion injury. Sci Rep 6: 24498, 2016.
42. Shi X, Wang J, Lei Y, Cong C, Tan D and Zhou X: Research progress on the PI3K/AKT signaling pathway in gynecological cancer (Review). Mol Med Rep 19: 4529-4535, 2019.
43. Ajzashokouhi AH, Rezaee R, Omidkhoda N and Karimi G: Natural compounds regulate the PI3K/Akt/GSK3β pathway in myocardial ischemia-reperfusion injury. Cell Cycle 22: 741-757, 2023.
44. Maciel L, de Oliveira D, Mesquita F, Souza HADS, Oliveira L, Christie MLA, Palhano FL, Campos de Carvalho AC, Nascimento JHM and Foguel D: New cardiomyokine reduces myocardial ischemia/reperfusion injury by PI3K-AKT pathway via a putative KDEL-receptor binding. J Am Heart Assoc 10: e019685, 2021.
45. Ghanaatfar F, Ghanaatfar A, Isapour P, Farokhi N, Bozorgniahosseini S, Javadi M, Gholami M, Ulloa L, Coleman-Fuller N and Motaghinejad M: Is lithium neuroprotective? An updated mechanistic illustrated review. Fundam Clin Pharmacol 37: 4-30, 2023.
46. Reis CR, Chen PH, Srinivasan S, Aguet F, Mettlen M and Schmid SL: Crosstalk between Akt/GSK3β signaling and dynamin-1 regulates clathrin-mediated endocytosis. EMBO J 34: 2132-2146, 2015.
47. Du H, Jin X, Jin S, Zhang D, Chen Q, Jin X, Wang C, Qian G and Ding H: Anti-leukemia activity of polysaccharide from Sargassum fusiforme via the PI3K/AKT/BAD pathway in vivo and in vitro. Mar Drugs 21: 289, 2023.
48. Akbari G: Role of zinc supplementation on ischemia/reperfusion injury in various organs. Biol Trace Elem Res 196: 1-9, 2020.
49. Ye Y, Xiaoyang C, Junkai Y, Yueyao HU and Wei W: Efficacy of Danlou tablet on myocardial ischemia/reperfusion injury assessed by network pharmacology and experimental verification. J Tradit Chin Med 44: 131-144, 2024.
50. Liu L, Zhang Y, Du Y, Li H, Wang M and Lv J: The therapeutic effect and targets of cellulose polysaccharide on coronary heart disease (CHD) and the construction of a prognostic signature based on network pharmacology. Front Nutr 9: 986639, 2022.
51. Liu C, Zhao W, Su J, Chen X, Zhao F, Fan J, Li X, Liu X, Zou L, Zhang M, *et al*: HSP90AA1 interacts with CSFV NS5A protein and regulates CSFV replication via the JAK/STAT and NF-κB signaling pathway. Front Immunol 13: 1031868, 2022.